search.
(46) (a) B.-K. Teo, M. B. Hall, R. F. Fenske, and L. F. Dahl, *J. Organomet. Chem.*, **70**, 413 (1974); (b) B.-K. Teo, Ph.D. Thesis, University of Wisconsin—Madison, 1973.
(47) C. F. Campana, Ph.D. Thesis, University of Wisconsin—Madison, 1975, C. F. Campana and L. F. Dahl, to be published.
(48) (a) B. Metz, D. Moras, and R. Weiss, *Chem. Commun.*, 444 (1971); (b) D. Moras, B. Metz, and R. Weiss, *Acta Crystallogr., Sect. B*, **29**, 383 (1973); (c) *ibid.*, **29**, 388 (1973); (d) D. Moras and R. Weiss, *ibid.*, **29**, 396 (1973); (e) *ibid.*, **29**, 400 (1973); (f) F. J. Tehan, B. L. Barnett, and J. L. Dye, *J. Am. Chem. Soc.*, **96**, 7203 (1974); (g) D. G. Adolphson, J. D. Corbett, and D. J. Merryman, *ibid.*, **98**, 7234 (1976); (h) R. G. Teller, R. G. Finke, J. P. Collman, H. B. Chin, and R. Bau, *ibid.*, **99**, 1104 (1977).
(49) (a) M. B. Hall and R. F. Fenske, *Inorg. Chem.*, 11, 768 (1972); (b) R. F. Fenske, *Pure Appl. Chem.*, **27**, 61 (1971); (c) *Prog. Inorg. Chem.*, **21**, 179 (1976).
(50) Cf. R. S. Gall, C. Ting-Wah Chu, and L. F. Dahl, *J. Am. Chem. Soc.*, **96**, 4019 (1974).
(51) Cf. Trinh-Toan, B.-K. Teo, J. A. Ferguson, T. J. Meyer, and L. F. Dahl, *J. Am. Chem. Soc.*, **99**, 408 (1977), and references cited therein.
(52) Cf. (a) Boon-Keng Teo and J. C. Calabrese, *J. Am. Chem. Soc.*, **97**, 1256 (1975); (b) *Inorg. Chem.*, **15**, 2467, 2474 (1976); (c) M. R. Churchill, J. Donahue, and F. J. Rotella, *ibid.*, **15**, 2752 (1976); (d) M. R. Churchill, B. G. DeBoer, and S. J. Mendak, *ibid.*, **14**, 2041 (1975); (e) M. R. Churchill, B. G. DeBoer, and D. J. Donovan, *ibid.*, **14**, 617 (1975).
(53) W. G. Klemperer, *J. Am. Chem. Soc.*, **94**, 8360 (1972).

Demonstration of the Generality of the $[Fe_4S_4(SR)_4]^{2-}$ (Compressed D_{2d})/$[Fe_4S_4(SR)_4]^{3-}$ (Elongated D_{2d}) Structural Change in Electron-Transfer Reactions of Ferredoxin 4-Fe Site Analogues. A Model for Unconstrained Structural Changes in Ferredoxin Proteins

Edward J. Laskowski,[1a] John G. Reynolds,[1a] Richard B. Frankel,*[1b] S. Foner,[1b] G. C. Papaefthymiou,[1b] and R. H. Holm*[1a]

Contribution from the Department of Chemistry, Stanford University, Stanford, California 94305, and the Francis Bitter National Magnet Laboratory, Massachusetts Institute of Technology, Cambridge, Massachusetts 02139.
Received April 4, 1979

Abstract: The ^{57}Fe Mössbauer, magnetic susceptibility, magnetization, and EPR properties of an extensive series of $(R_4'N)_3[Fe_4S_4(SR)_4]$ compounds (R = Ph, *o*-, *m*-, *p*-C_6H_4Me, *p*-C_6H_4-*i*-Pr, CH_2Ph, CH_2-*p*-C_6H_4OMe) have been examined in the solid state and in frozen acetonitrile solutions. The cluster trianions serve as analogues of the sites of Fd_{red} proteins. Based on similarities and differences in their properties in the solid state the compounds divide into two categories: those whose $[Fe_4S_4(SR)_4]^{3-}$ clusters contain tetragonal or nontetragonal Fe_4S_4 core structures. The lack of core structural uniformity is attributed to perturbing influences in the solid state. Irrespective of their solid-state category all compounds in frozen solution exhibit essentially coincident properties (most thoroughly documented by EPR and Mössbauer spectral results), which are indicative of a single core structure of a set of closely related core structures. From a previous demonstration of the similarity of properties of $[Fe_4S_4(SPh)_4]^{3-}$ salts in the solid and solution state and the X-ray structure of this cluster, the solution core structure of the set of cluster trianions is identified as elongated tetragonal. These findings, together with the previously established high degree of core structural uniformity in the Fd_{ox} analogues $[Fe_4S_4(SR)_4]^{2-}$, provide substantial experimental support for two proposals: (1) an elongated (idealized) D_{2d} core structure is the intrinsically stable configuration of $[Fe_4S_4(SR)_4]^{3-}$; (2) the unconstrained idealized core structural change accompanying electron transfer is $[Fe_4S_4(SR)_4]^{2-}$ (compressed D_{2d}) $\rightleftharpoons$ $[Fe_4S_4(SR)_4]^{3-}$ (elongated D_{2d}). This process serves as a representation of protein site structural changes in a Fd_{ox}/Fd_{red} electron transfer couple in the absence of extrinsic constraints such as might be imposed by protein structural features.

Introduction

Previous experiments have firmly established the following isoelectronic relationships between the $[Fe_4S_4(S\text{-}Cys)_4]$ sites in ferredoxin (Fd) proteins and synthetic clusters: $Fd_{ox} \equiv [Fe_4S_4(SR)_4]^{2-}$,[2,3] $Fd_{red} \equiv [Fe_4S_4(SR)_4]^{3-}$.[3-6] Following the earlier synthesis of the cluster dianions,[2,3,7] the recent preparation of cluster trianions[4] has provided access to analogues of the sites of both members of the Fd_{ox}/Fd_{red} redox couple, which has been implicated in electron-transport chains to numerous oxidoreductase enzymes.[8] Further, there is substantial evidence in some cases (e.g., trimethylamine dehydrogenase,[9] hydrogenase,[10] FeMo proteins of nitrogenase[11]) and a definite possibility with other Fe-S enzymes[8] that one or more Fe_4S_4 units are contained within the enzyme structure and, in such instances, may function in internal electron transfer to and from catalytic sites. An ultimately satisfactory interpretation of the operation of any biological redox site, in terms of its rates and potentials of electron transfer, minimally requires accurate structural definition of the site in both oxidation levels of the redox couple in question. Although the structures of *Peptococcus aerogenes* Fd_{ox}[12] (two Fe_4S_4 units) and the reduced *Chromatium* "high-potential" protein[12b,c] (HP_{red}, one Fe_4S_4 unit isoelectronic with those in Fd_{ox}) have been solved to 2 Å resolution, there is at present no structural data from X-ray diffraction on any Fd_{red} protein. Very recent EXAFS studies[13] have verified the close structural similarity between Fd_{ox}, HP_{red}, and $[Fe_4S_4(SR)_4]^{2-}$, consistent with results from diffraction investigations,[2,7,12] and have revealed small changes (<0.1 Å) in mean Fe-S and Fe · · · Fe distances in the two oxidation levels of a bacterial Fd. However, this method is insufficiently precise to localize the small structural differences observed.

Our approach to elucidation of structures of and structural differences between 4-Fe redox sites is based on the use of the synthetic analogues $[Fe_4S_4(SR)_4]^{2-,3-}$; pertinent findings are summarized in Figure 1. The Fd_{ox} site analogues $[Fe_4S_4(SR)_4]^{2-}$ (R = CH_2Ph,[7] Ph[14]), with the $[Fe_4S_4]^{2+}$ *core*

0002-7863/79/1501-6562$01.00/0

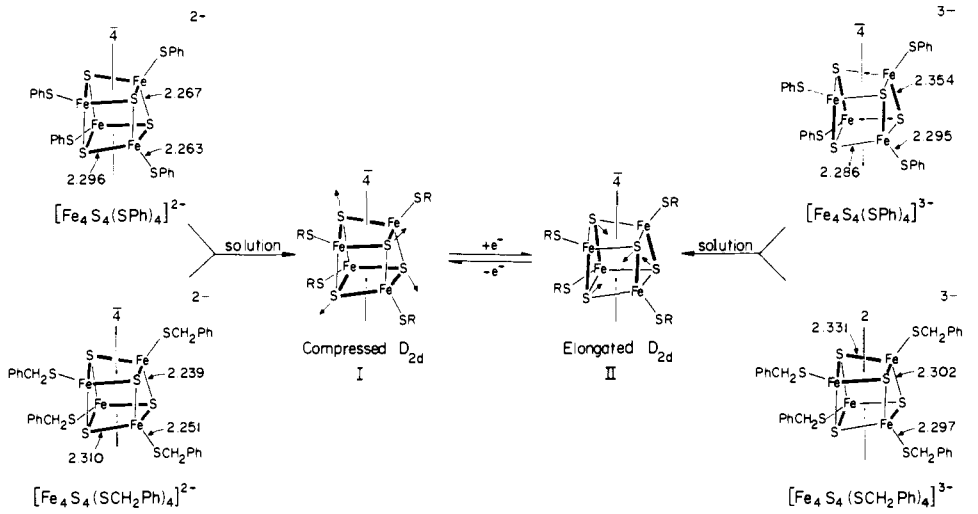

Figure 1. Structures of $[Fe_4S_4(SPh)_4]^{2-,3-}$ and $[Fe_4S_4(SCH_2Ph)_4]^{2-,3-}$ in the crystalline state and a simplified representation of the structural interconversion of the Fe_4S_4 core pursuant to $[Fe_4S_4(SR)_4]^{2-,3-}$ electron transfer in solution. Idealized core symmetry axes and mean values of Fe-SR and sets of longer (dark lines) and shorter Fe-S bonds are shown.

oxidation level, exhibit idealized tetragonal core geometry *compressed* along the $\bar{4}$ axis. Inasmuch as Fd_{ox} and HP_{red} sites exhibit a similar core distortion from T_d symmetry,[12] as do other closely related clusters with the same core oxidation level,[15] there can be little question that a compressed D_{2d} core configuration is the intrinsically stable form of this oxidation level. The situation with the Fd_{red} site analogues $[Fe_4S_4(SR)_4]^{3-}$, having the $[Fe_4S_4]^{+}$ core oxidation level, does not appear to be as straightforward. In its Et_3MeN^+ salt $[Fe_4S_4(SPh)_4]^{3-}$ possesses an idealized tetragonal core geometry *elongated* along the $\bar{4}$ axis,[6] whereas $[Fe_4S_4(SCH_2Ph)_4]^{3-}$ in its Et_4N^+ salt exhibits a less regular core configuration with idealized C_{2v} symmetry.[16] Spectroscopic and magnetic properties of these two crystalline salts are significantly different,[6] reflecting the structural differences of the two clusters. However, in solution these properties are essentially coincident and are not significantly different from those of $[Fe_4S_4(SPh)_4]^{3-}$ in the solid state.[6] These observations have led to two proposals:[6] (1) an elongated D_{2d} core structure is the intrinsically stable configuration of $[Fe_4S_4(SR)_4]^{3-}$ clusters; (2) the structural change pursuant to electron transfer in the absence of extrinsic constraints such as might be imposed by crystal packing forces or protein structural features may be reasonably represented by I $\rightleftharpoons$ II in Figure 1.

The foregoing proposals, while founded on a substantial body of experiments,[6] were offered on the basis of observations of only two Fd_{red} site analogues $[Fe_4S_4(SR)_4]^{3-}$, R = Ph and CH_2Ph. In this report we provide the results of an extensive investigation of certain physicochemical properties (Mössbauer and EPR spectral features, magnetic susceptibilities, and magnetization) of a larger series of $[Fe_4S_4(SR)_4]^{3-}$ clusters. The principal intent of this work is to provide an assessment of the general viability of proposals (1) and (2) and their relation to electron-transfer processes of biological 4-Fe sites.

Experimental Section

Preparation of Compounds. *p-tert*-Butylbenzenethiol[17] and *p*-isopropylbenzenethiol[18] were obtained by published methods; *p*-methoxybenzylthiol was a commercial product (Aldrich Chemical Co.). All operations were carried out under a N_2/Ar atmosphere. New dianions of the type $[Fe_4S_4(SR)_4]^{2-}$ (R = CH_2-*p*-C_6H_4OMe, *p*-C_6H_4-*i*-Pr, *p*-C_6H_4-*t*-Bu) were prepared by the method of direct tetramer synthesis[7] and were isolated as quaternary ammonium salts, which were purified by recrystallization from acetonitrile–methanol. These compounds are intensely colored and air sensitive.

$(Et_4N)_2[Fe_4S_4(SCH_2$-*p*-$C_6H_4OMe)_4]$. Anal. Calcd for $C_{48}H_{76}Fe_4N_2O_4S_8$: C, 47.06; H, 6.25; N, 2.29; S, 20.94. Found: C, 46.93; H, 6.14; N, 2.34; S, 20.97. Green-black solid.

$(Et_4N)_2[Fe_4S_4(S$-*p*-C_6H_4-*i*-Pr$)_4]$. Anal. Calcd for $C_{52}H_{84}Fe_4N_2S_8$: C, 51.31; H, 6.96; N, 2.30; S, 21.08. Found: C, 51.40; H, 7.03; N, 2.29; S, 21.11. Red-black solid.

$(Et_4N)_2[Fe_4S_4(S$-*p*-C_6H_4-*t*-Bu$)_4]$. Anal. Calcd for $C_{56}H_{92}Fe_4N_2S_8$: C, 52.83; H, 7.28; N, 2.20; S, 20.15. Found: C, 52.60; H, 7.04; N, 2.22; S, 20.08. Red-black solid.

The trianion salts $(Et_4N)_3[Fe_4S_4(SR)_4]$ (R = CH_2-*p*-C_6H_4OMe, *p*-C_6H_4-*i*-Pr) were synthesized by the reduction of the corresponding dianion salt with sodium acenaphthalenide in hexamethylphosphoramide. The procedure used was that of Cambray et al.[4] with the following modifications. The reducing agent was added over a period of 30 s. The reaction was allowed to proceed for 2 h under vacuum at room temperature, at which time THF was vacuum transferred into the reaction mixture cooled to 0 °C. The crude product which separated was collected and purified by recrystallization under vacuum from acetonitrile–THF solutions at 0 °C. The pure compounds were obtained as extremely air-sensitive, greenish-black crystals.

$(Et_4N)_3[Fe_4S_4(SCH_2$-*p*-$C_6H_4OMe)_4]$. Anal. Calcd for $C_{56}H_{96}Fe_4N_3O_4S_8$: C, 49.63; H, 7.14; N, 3.10; S, 18.93. Found: C, 49.53; H, 7.06; N, 3.17; S, 18.90.

$(Et_4N)_3[Fe_4S_4(S$-*p*-C_6H_4-*i*-Pr$)_4]$. Anal. Calcd for $C_{60}H_{104}Fe_4N_3S_8$: C, 53.49; H, 7.78; N, 3.12; S, 19.04. Found: C, 53.54; H, 7.75; N, 2.93; S, 18.88.

Salts of $[Fe_4S_4(SR)_4]^{3-}$ with R = Et and *p*-C_6H_4-*t*-Bu were not obtained in satisfactory analytical purity. Those with R = Ph, CH_2Ph, *o*-C_6H_4Me, *m*-C_6H_4Me, and *p*-C_6H_4Me were available from previous investigations in this laboratory.[6,19]

Physical Measurements. ^{57}Fe Mössbauer spectra were obtained at 77 and 4.2 K in zero magnetic field and in longitudinally applied magnetic fields H_0 up to 80 kOe at 4.2 K. The ^{57}Co in Rh metal source was maintained at the same temperature as the absorbers. The latter were prepared under dry dinitrogen by mixing salts of $[Fe_4S_4(SR)_4]^{3-}$ with boron nitride to avoid preferential alignment of the crystallites and sealing into plastic absorber holders, which were immediately immersed in liquid nitrogen. The absorbers were kept cold during transfer into the spectrometer and during all the subsequent measurements. Absorbers consisting of frozen ~30 mM acetonitrile solutions were also prepared by dissolving the appropriate salt in acetonitrile under dry dinitrogen, sealing into plastic holders, and freezing in liquid nitrogen. The solutions were kept frozen for all subsequent operations and measurements. Magnetic susceptibility determinations at 2 kG and EPR measurements were made using the procedures and instrumentation previously described.[6] Magnetization measurements of solid samples were made at 4.2 and 1.45 K over an external magnetic field range of zero to 57 kOe using the vibrating sample magnetometer adapted to a superconducting solenoid. Sample weights of ca. 30–50 mg were used and samples were measured in thin-walled Delrin or Kel-F containers.

Table I. Mössbauer Parameters for $[Fe_4S_4(SR)_4]^{3-}$ Clusters at 4.2 K

compd	solid state		CH_3CN solution	
	δ, mm/s[a]	ΔE_Q, mm/s[b]	δ, mm/s[a]	ΔE_Q, mm/s[b]
$(Et_4N)_3[Fe_4S_4(SPh)_4]$[c]	0.52	2.04	0.51	2.01
	0.45	1.13	0.46	1.11
$(Me_4N)_3[Fe_4S_4(S\text{-}o\text{-}C_6H_4Me)_4]$	0.50	1.93	0.54	1.67
	0.43	1.09	0.44	1.02
$(Me_4N)_3[Fe_4S_4(S\text{-}m\text{-}C_6H_4Me)_4]$	0.45[d]	1.01	0.53	1.70
			0.44	0.99
$(Me_4N)_3[Fe_4S_4(S\text{-}p\text{-}C_6H_4Me)_4]$	0.43[d]	1.06	0.53	1.70
			0.45	0.99
$(Et_4N)_3[Fe_4S_4(S\text{-}p\text{-}C_6H_4\text{-}i\text{-}Pr)_4]$	0.44[d]	1.01	0.50	1.90
			0.45	1.06
$(Et_4N)_3[Fe_4S_4(SCH_2Ph)_4]$[c]	0.48	1.41	0.52	2.01
	0.48	0.93	0.47	1.12
$(Et_4N)_3[Fe_4S_4(SCH_2\text{-}p\text{-}C_6H_4OMe)_4]$	0.43[d]	0.86	0.50	1.90
			0.45	1.06

[a] ±0.02 mm/s; relative to Fe metal at 4.2 K. To convert these values to Fe metal at room temperature, add 0.12 mm/s. [b] ±0.03 mm/s. [c] Data from ref 6 corrected to refer to Fe metal at 4.2 K. [d] Fit assuming one quadrupole doublet.

Table II. EPR and Magnetic Data for $[Fe_4S_4(SR)_4]^{3-}$ Clusters at 4.2 K

compd	solid	solution		
	μ_t,[a] μ_B (4.2 K)	solvent	μ_t, μ_B (4.2 K)	g values[b]
$(Et_4N)_3[Fe_4S_4(SPh)_4]$[c]	2.05	CH_3CN	2.10	2.06, 1.93[d]
$(Et_3MeN)_3[Fe_4S_4(SPh)_4]$[c]	2.03	DMF		2.06, 1.93
$(Me_4N)_3[Fe_4S_4(S\text{-}o\text{-}C_6H_4Me)_4]$	2.52	DMF		2.06, 1.92
$(Me_4N)_3[Fe_4S_4(S\text{-}m\text{-}C_6H_4Me)_4]$	3.58	DMF		2.06, 1.93
$(Me_4N)_3[Fe_4S_4(S\text{-}p\text{-}C_6H_4Me)_4]$	3.15	DMF		2.04, 1.93
$(Et_4N)_3[Fe_4S_4(S\text{-}p\text{-}C_6H_4\text{-}i\text{-}Pr)_4]$	3.40	CH_3CN		2.05, 1.92
$(Et_4N)_3[Fe_4S_4(SCH_2Ph)_4]$[c]	3.35	CH_3CN	2.09	2.04, 1.93
$(n\text{-}Pr_4N)_3[Fe_4S_4(SCH_2Ph)_4]$[c]	2.60			2.04, 1.93
$(Et_4N)_3[Fe_4S_4(SCH_2\text{-}p\text{-}C_6H_4OMe)_4]$	3.85	CH_3CN	2.29	2.02, 1.93

[a] Magnetic moment per 4 Fe atoms of tetrameric (t) unit; calculated as in Table III. [b] Determined at ~4.2 K. [c] Data from ref 6. [d] DMF solution.

Results

The reduced clusters $[Fe_4S_4(SR)_4]^{3-}$ with R = *o*-, *m*-, *p*-C_6H_4Me, *p*-C_6H_4-*i*-Pr, and CH_2-*p*-C_6H_4OMe have been investigated in this work. Their selection was dictated by several considerations. First, although the sodium acenaphthylenide reduction procedure[4] applied to $[Fe_4S_4(SR)_4]^{2-}$ complexes with a variety of R = alkyl and substituted phenyl substituents affords the corresponding trianions (as shown by EPR measurements), it has not yet proven possible to *isolate* in satisfactory analytical purity trianions for which $E_{1/2}(2-/3-) < -1.3$ V in DMF.[20] Such species are extraordinarily sensitive to oxidation, a most unfavorable property when the only purification method requires several recrystallizations. Consequently, the only acceptably pure trianion salts thus far obtained are those with R = Ph, CH_2Ph, and their substituted variants. Second, the differences in structures (Figure 1) and Mössbauer and magnetic properties (Tables I and II) between salts of $[Fe_4S_4(SPh)_4]^{3-}$ and $[Fe_4S_4(SCH_2Ph)_4]^{3-}$ and between two different salts of the latter trianion indicate, as concluded elsewhere,[6,16] that solid-state environmental effects are primarily responsible for these differences. Accordingly, the specified substituent variations on R = Ph and CH_2Ph might also reflect the existence of these effects without imposing large electronic perturbations on the clusters. In this way a more direct comparison of the newer results with those for $[Fe_4S_4(SPh)_4]^{3-}$ and $[Fe_4S_4(SCH_2Ph)_4]^{3-}$ is obtained than would be the case for other potentially isolable $[Fe_4S_4(SR)_4]^{3-}$ salts with electronically and structurally different R substituents.

In the sections which follow, certain spectroscopic and magnetic properties of cluster trianions are employed where possible as diagnostic indicators of structures and structural differences in the solid state and in solution. Trianion salts have proven difficult to crystallize in forms suitable for X-ray diffraction studies; structural information[6,16] is presently confined to that summarized in Figure 1. The understanding of oxidized and reduced clusters has not reached the point where the properties recorded here and elsewhere[4-6] can be satisfactorily interpreted in terms of electronic structures. However, preliminary energy level diagrams[21] and models of spin-coupled clusters for interpretation of Mössbauer and EPR spectra[22] have been presented.

Mössbauer Spectra. Parameters obtained from computer fitting[6] of the spectra of $[Fe_4S_4(SR)_4]^{3-}$ clusters observed in the solid state and in acetonitrile solution at 4.2 K are collected in Table I together with previous data for $[Fe_4S_4(SPh)_4]^{3-}$ and $[Fe_4S_4(SCH_2Ph)_4]^{3-}$.

A. Polycrystalline Solids. Spectra of the series of $(Me_4N)_3[Fe_4S_4(SC_6H_4Me)_4]$ salts in zero applied magnetic field are shown in Figure 2. For $[Fe_4S_4(S\text{-}o\text{-}C_6H_4Me)_4]^{3-}$ the spectrum (Figure 2a) consists of two overlapping quadrupole doublets with different isomer shifts (δ) and quadrupole splittings (ΔE_Q) and different line widths, indicating magnetic hyperfine relaxation effects. The relative intensities of the two doublets are ca. 1:1; quadrupole splittings decrease as the temperature is increased to 77 K. Spectra of this compound in externally applied magnetic fields can be characterized as follows. For $0 < H_0 \leq 40$ kOe, the spectrum broadens but is not resolved. For $40 < H_0 \leq 80$ kOe, in addition to an unresolved absorption area in the center of the spectrum, two moderately well resolved pairs of lines flanking this area are observed. The $H_0 = 80$ kOe spectrum is shown in Figure 3a. One pair of lines exhibits a splitting which decreases with increasing H_0 while the splitting of the other pair increases with increasing H_0. This behavior indicates at least two magneti-

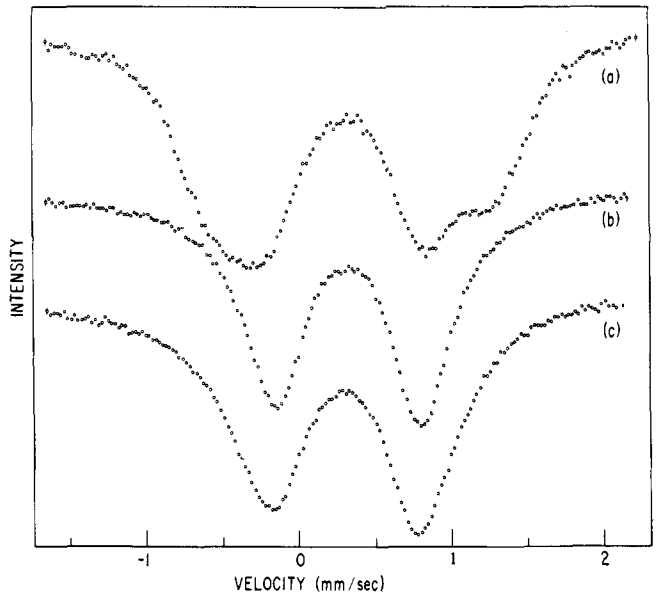

Figure 2. Mössbauer spectra of $(Me_4N)_3[Fe_4S_4(SR)_4]$ in the solid state at 4.2 K ($H_0 = 0$): (a) R = o-C_6H_4Me; (b) R = m-C_6H_4Me; (c) R = p-C_6H_4Me.

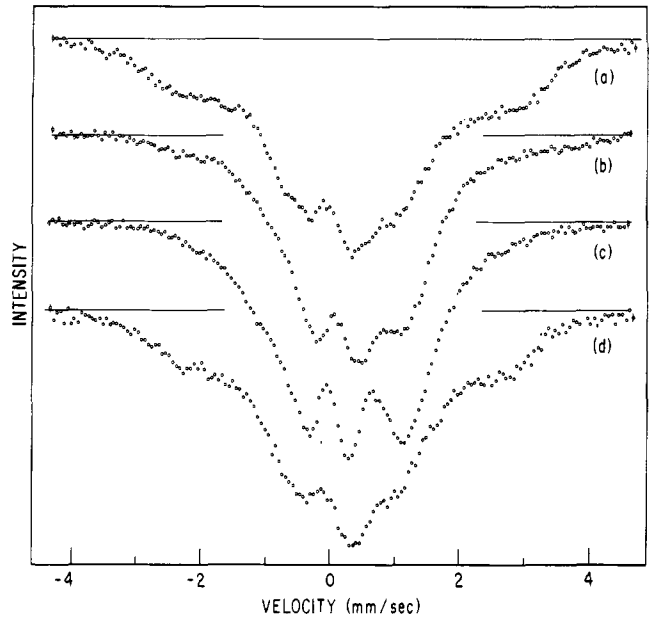

Figure 3. Mössbauer spectra of $(Me_4N)_3[Fe_4S_4(SR)_4]$ at 4.2 K and H_0 = 80 kOe: (a) R = o-C_6H_4Me, solid; (b) R = m-C_6H_4Me, solid; (c) R = p-C_6H_4Me, solid; (d) R = p-C_6H_4Me, ~30 mM acetonitrile solution.

cally inequivalent sites (as does the zero-field spectrum) and internal magnetic fields at the Fe nuclei which are different from the applied fields. The magnetic hyperfine interaction constants estimated from the observed splittings are different for the two sites, implying different electron spin densities at these sites.[23] As shown by the magnetic and EPR data in Tables II and III, $[Fe_4S_4(S\text{-}o\text{-}C_6H_4Me)_4]^{3-}$ and all other trianions are paramagnetic at $T \geq 4.2$ K. The Mössbauer spectral properties of $[Fe_4S_4(S\text{-}o\text{-}C_6H_4Me)_4]^{3-}$ in zero and applied magnetic fields much more closely resemble those of $[Fe_4S_4(SPh)_4]^{3-}$ than those of $[Fe_4S_4(SCH_2Ph)_4]^{3-}$ (Table I). In particular, the presence of two quadrupole doublets is clearly evident in the $H_0 = 0$ spectra of the first two clusters and their ΔE_Q values are quite similar.

For the remaining trianions $[Fe_4S_4(SR)_4]^{3-}$, with R = m-C_6H_4Me, p-C_6H_4Me, p-C_6H_4-i-Pr, and CH_2-p-C_6H_4OMe, the $H_0 = 0$ solid state spectra consist of a quadrupole doublet with broadened lines and quadrupole splittings which decrease as the temperature is increased to 77 K. Spectra of the first two species are set out in Figures 2b and 2c. The observed line broadening could result from unresolved inequivalence of Fe sites and/or magnetic hyperfine relaxation effects. Applied magnetic fields up to 80 kOe induce magnetic hyperfine interactions but in all cases the overall splittings are less than ca. 40% of those observed with $[Fe_4S_4(S\text{-}o\text{-}C_6H_4Me)_4]^{3-}$ under the same conditions. This behavior is illustrated for the R = m- and p-C_6H_4Me trianions in Figures 3b and 3c and for the R = p-C_6H_4-i-Pr and CH_2-p-C_6H_4OMe trianions in Figure 4. The overall splitting changes from species to species signify different magnetic hyperfine interactions produced by the combined effects of different R substituents and whatever structural differences occur among the members of this set of four trianions in the solid state. The Mössbauer features of this set are more closely similar to the properties of $[Fe_4S_4(SCH_2Ph)_4]^{3-}$ than to those of $[Fe_4S_4(SPh)_4]^{3-}$ and $[Fe_4S_4(S\text{-}o\text{-}C_6H_4Me)_4]^{3-}$. Particular points of similarity include broadened quadrupole doublets in the $H_0 = 0$ spectra and substantially reduced magnetic hyperfine interactions compared to the latter two trianions.

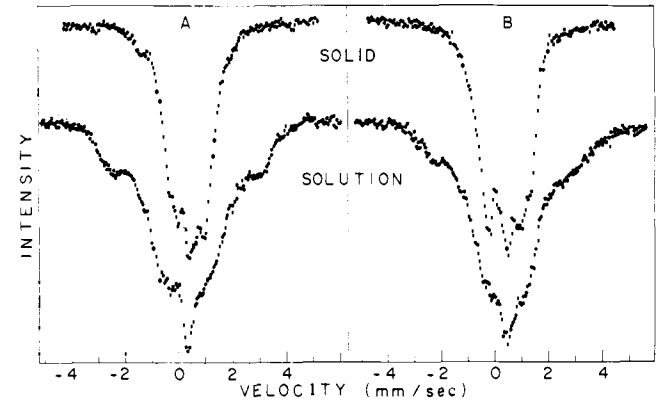

Figure 4. Mössbauer spectra of $(Et_4N)_3[Fe_4S_4(SR)_4]$ in the solid state and in frozen acetonitrile solution at 4.2 K and H_0 = 80 kOe: A, R = CH_2-p-C_6H_4OMe; B, R = p-C_6H_4-i-Pr.

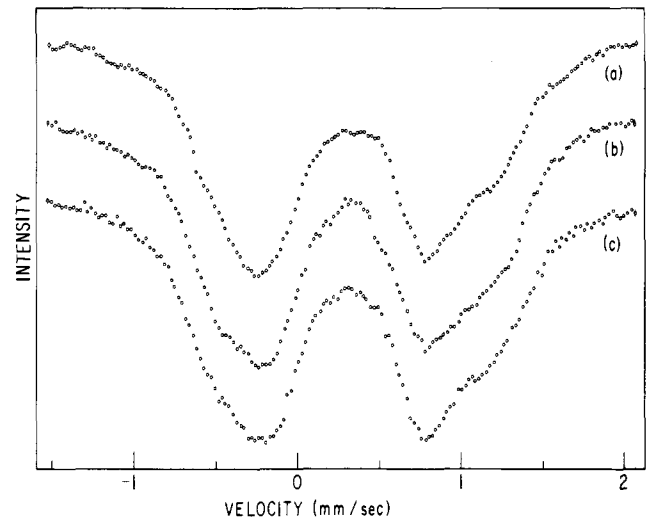

Figure 5. Mössbauer spectra of ~30 mM solutions of $(Me_4N)_3[Fe_4S_4(SR)_4]$ in acetonitrile at 4.2 K ($H_0 = 0$): (a) R = o-C_6H_4Me; (b) R = m-C_6H_4Me; (c) R = p-C_6H_4Me.

B. Frozen Solutions. Spectra of the three members of the $[Fe_4S_4(SC_6H_4Me)_4]^{3-}$ series in acetonitrile solution at H_0 = 0 and 4.2 K are presented in Figure 5. Each spectrum consists of at least two overlapping quadrupole doublets. The marked

Table III. Magnetic Data for $[Fe_4S_4(SR)_4]^{3-}$ Clusters in the Solid State at Selected Temperatures

	$(Me_4N)_3[Fe_4S_4(S\text{-}o\text{-}C_6H_4Me)_4]$		$(Me_4N)_3[Fe_4S_4(S\text{-}m\text{-}C_6H_4Me)_4]$	
T, K	$\chi_t \times 10^3$ [a]	μ_t, μ_B [b]	$\chi_t \times 10^3$	μ_t, μ_B
4.2	189	2.52	382	3.58
10.6	86.6	2.71	165	3.74
19.7	52.0	2.86	90.7	3.78
29.8	37.7	3.00	61.8	3.84
40.4	29.5	3.09	46.2	3.86
50.4	24.4	3.14	36.4	3.83
60.3	21.0	3.18	30.8	3.85
70.1	18.8	3.25	26.5	3.85
80.2	17.1	3.31	23.8	3.91
90.2	16.0	3.39	21.3	3.92
100.2	14.7	3.43	19.7	3.97
150.3	11.6	3.73		

	$(Me_4N)_3[Fe_4S_4(S\text{-}p\text{-}C_6H_4Me)_4]$		$(Et_4N)_3[Fe_4S_4(S\text{-}p\text{-}C_6H_4\text{-}i\text{-}Pr)_4]$	
T, K	$\chi_t \times 10^3$	μ_t, μ_B	$\chi_t \times 10^3$	μ_t, μ_B
4.2	296	3.15	344	3.40
10.6	135	3.38	152	3.59
19.7	75.5	3.45	82.2	3.60
29.8	50.7	3.48	56.3	3.66
40.4	37.6	3.49	41.0	3.64
50.4	29.2	3.43	32.0	3.59
60.3	24.7	3.45	26.9	3.60
70.1	21.7	3.49	23.3	3.61
80.2	19.1	3.50	20.4	3.62
90.2	17.3	3.53	18.3	3.63
100.2	16.1	3.59	16.8	3.67
150.3	12.0	3.80	12.5	3.88
200.3	10.2	4.04	10.6	4.12
298.9	8.45	4.49	8.70	4.56

	$(Et_4N)_3[Fe_4S_4(SCH_2\text{-}p\text{-}C_6H_4OMe)_4]$	
T, K	$\chi_t \times 10^3$	μ_t, μ_B
4.2	441	3.85
10.6	174	3.84
19.7	93.0	3.83
29.8	63.1	3.88
40.4	47.7	3.93
50.4	38.7	3.95
60.3	33.4	4.01
70.1	29.5	4.07
80.2	27.0	4.16
90.2	24.9	4.24
100.2	22.4	4.24
150.3	16.6	4.47
200.3	13.2	4.60
298.9	10.5	4.01

[a] Per 4 Fe atoms of tetranuclear (t) cluster, corrected for diamagnetism. [b] $\mu_t = 2.828(\chi_t T)^{1/2}$; $\mu_{Fe} = \mu_t/2$.

similarity among these spectra and between them and the spectrum of $[Fe_4S_4(S\text{-}o\text{-}C_6H_4Me)_4]^{3-}$ in the solid state (Figure 2a) is readily apparent, as are the spectral differences with the solid absorbers $[Fe_4S_4(SR)_4]^{3-}$ (R = *m*-, *p*-C_6H_4Me; Figures 2b and 2c). The spectra in Figure 3, recorded at H_0 = 80 kOe, provide further demonstration of this behavior. The spectra of $[Fe_4S_4(S\text{-}p\text{-}C_6H_4Me)_4]^{3-}$ in solution and $[Fe_4S_4(S\text{-}o\text{-}C_6H_4Me)_4]^{3-}$ in the solid state are more closely related than is either spectrum with those of $[Fe_4S_4(SR)_4]^{3-}$ (R = *m*-, *p*-C_6H_4Me) in polycrystalline form. Further, the H_0 = 80 kOe solution spectra at 4.2 K of $[Fe_4S_4(SCH_2\text{-}p\text{-}C_6H_4OMe)_4]^{3-}$ and $[Fe_4S_4(S\text{-}p\text{-}C_6H_4\text{-}i\text{-}Pr)_4]^{3-}$ in Figure 4 reveal clear similarities to each other and to that of $[Fe_4S_4(S\text{-}p\text{-}C_6H_4Me)_4]^{3-}$ (Figure 3d) under the same conditions.

The parameters of the solution spectra, assembled in Table I and obtained by assuming two quadrupole doublets with Lorentzian line shapes, provide quantitative measure of the similarity of all such spectra. The higher and lower velocity quadrupole doublets have the parameters δ = 0.50–0.54, ΔE_Q = 1.67–2.01 mm/s and δ = 0.44–0.47, ΔE_Q = 0.99–1.12 mm/s, respectively. From the criterion of Mössbauer spectral similarities we conclude that all other $[Fe_4S_4(SR)_4]^{3-}$ clusters in acetonitrile solution adopt a structure, or a small range of structures, such that their Fe atoms are virtually indistinguishable electronically from those in $[Fe_4S_4(SPh)_4]^{3-}$ and $[Fe_4S_4(S\text{-}o\text{-}C_6H_4Me)_4]^{3-}$ in the solid and solution states.

Magnetic Properties. Two types of properties were examined: magnetic susceptibilities in the solid state and, for one compound, in acetonitrile solution over the minimum temperature interval of 4.2–100 K, with some measurements extended to 337 K; magnetization in the solid state at 4.2 K and at applied fields H_0 up to 54 kOe. Magnetic susceptibilities of salts of $[Fe_4S_4(SPh)_4]^{3-}$ and $[Fe_4S_4(SCH_2Ph)_4]^{3-}$ in the solid state and in frozen and fluid acetonitrile solution have been described at length elsewhere.[6,19] No magnetization results for $[Fe_4S_4(SR)_4]^{3-}$ clusters have been reported previously.

A. Magnetic Susceptibilities. Abbreviated magnetic data sets for the five new $[Fe_4S_4(SR)_4]^{3-}$ cluster salts examined in this investigation are given in Table III. Data presented are magnetic susceptibilities (χ_t) and magnetic moments (μ_t) per 4 Fe atoms of a tetranuclear (t) cluster. Plots of χ_t vs. T for four compounds in the solid state are presented in Figure 6. The data have not been corrected for any type of magnetic impurity. The most likely paramagnetic impurity is Fe(III), which, if present in magnetically dilute form, should be detectable by the appearance of a characteristic $g \sim 4.3$ EPR signal. Such signals are found to be very weak or absent in typical preparations of all compounds, a matter substantiated by the low-temperature solution spectra of four salts shown in Figure 7. General properties of all $[Fe_4S_4(SR)_4]^{3-}$ polycrystalline salts are magnetic moments at cryogenic temperatures in excess of those ($\sim$1.7 μ_B) calculated from g values (Table II), and decreasing susceptibilities and (excepting minor inversions) increasing moments with increasing temperature. Up to the highest temperature of measurement the latter two quantities greatly exceed those for a simple $S = \frac{1}{2}$ Ci paramagnet with $\mu \sim 1.7$ μ_B. Such behavior is consistent with antiferromagnetic spin coupling within the clusters.

Inspection of $\chi_t(T)$ data for nine compounds reveals that susceptibility differences are the most pronounced below $\sim$50 K. The magnetic moments at 4.2 K (Table II) correspond to the largest differences at any temperature and lead to the organization of compounds into two categories defined by their moments: 2.0–2.6 and 3.1–3.9 μ_B. Included in the first category are two salts of $[Fe_4S_4(SPh)_4]^{3-}$, one of which was used in the X-ray structure determination in Figure 1. The only new compound in this category is $(Me_4N)_3[Fe_4S_4(S\text{-}o\text{-}C_6H_4Me)_4]$. The remaining four new trianion salts fall into the second category together with $(Et_4N)_3[Fe_4S_4(SCH_2Ph)_4]$ (Figure 1), whose relatively high magnetic moment is no longer unique. As previously,[6] we regard the low-temperature magnetic variations to reflect structural differences in the solid state.[24] Clusters in compounds belonging to the first and second categories presumably possess or approach the elongated D_{2d} and less regular core geometries observed in $[Fe_4S_4(SPh)_4]^{3-}$ and $[Fe_4S_4(SCH_2Ph)_4]^{3-}$, respectively.

Susceptibility behavior of $(Et_4N)_3[Fe_4S_4(SCH_2\text{-}p\text{-}C_6H_4OMe)_4]$ in the solid state and in frozen acetonitrile solution is directly compared in Figure 6. This compound was selected on the basis of having the highest moment of all trianion salts in the solid state over the entire 4.2–337 K range. Results in the solid and solution phases are dramatically different. For example, at 4.2 and 150 K χ_t(solid) is nearly three

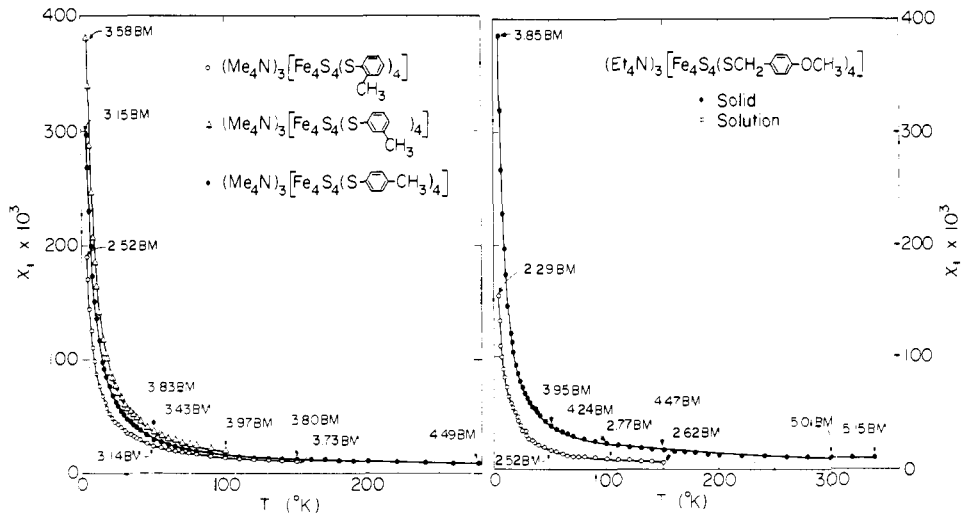

Figure 6. Temperature dependence of magnetic susceptibilities. Left: the three members of the $(Me_4N)_3[Fe_4S_4(SC_6H_4Me)_4]$ series in the solid state. Right: $(Et_4N)_3[Fe_4S_4(SCH_2\text{-}p\text{-}C_6H_4OMe)_4]$ in the solid state and in frozen acetonitrile solution. Magnetic moments at various temperatures are given. The smooth curves connecting the data points are meant only as guides to the location of these points.

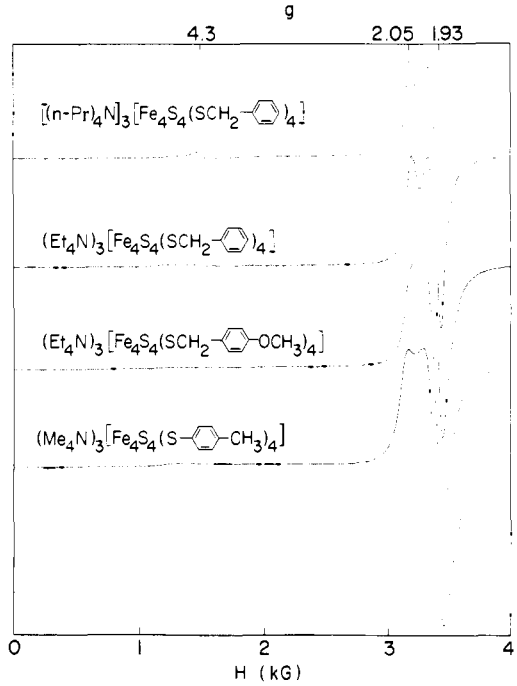

Figure 7. Frozen acetonitrile solution X-band EPR spectra of $[Fe_4S_4(SR)_4]^{3-}$ salts at 4.2 K recorded under the following conditions of solvent, modulation amplitude (G), microwave power (mW), and receiver gain: $[(n\text{-}Pr)_4N]_3[Fe_4S_4(SCH_2Ph)_4]$, CH_3CN, 10, 3, 1250; $(Et_4N)_3[Fe_4S_4(SCH_2Ph)_4]$, DMF, 12.5, 3, 2500; $(Et_4N)_3[Fe_4S_4(SCH_2\text{-}p\text{-}C_6H_4OMe)_4]$, CH_3CN, 20, 5, 63; $(Me_4N)_3[Fe_4S_4(S\text{-}p\text{-}C_6H_4Me)_4]$, DMF, 20, 5, 32. Solution concentrations were ca. 10^{-3} 10^{-4} M; the modulation frequency in all cases was 10^5 Hz.

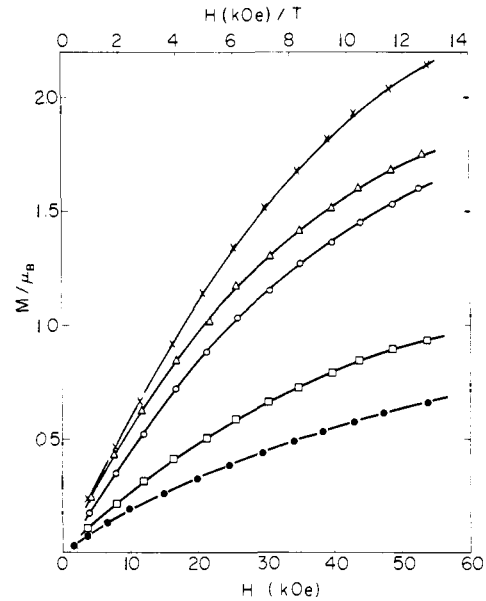

Figure 8. Magnetization per cluster (expressed in Bohr magnetons) as a function of magnetic field at 4.2 K for $[Fe_4S_4(SR)_4]^{3-}$ salts in the solid state: ●, $(Et_4N)_3[Fe_4S_4(SPh)_4]$; □, $(Me_4N)_3[Fe_4S_4(S\text{-}o\text{-}C_6H_4Me)_4]$; ○, $(Me_4N)_3[Fe_4S_4(S\text{-}p\text{-}C_6H_4Me)_4]$; △, $(Me_4N)_3[Fe_4S_4(S\text{-}m\text{-}C_6H_4Me)_4]$; ×, $(Et_4N)_3[Fe_4S_4(SCH_2Ph)_4]$.

times larger than χ_t(solution), with differences at intermediate temperatures only somewhat smaller. The solution magnetic data for three clusters in Table II correspond to χ_t values at 4.2 K which differ by ≤20%. Hence, by this magnetic criterion $[Fe_4S_4(SCH_2\text{-}p\text{-}C_6H_4OMe)_4]^{3-}$, which from Mössbauer and susceptibility results has an irregular structure in the solid state, possesses a solution configuration similar to those of $[Fe_4S_4(SPh)_4]^{3-}$ and $[Fe_4S_4(SCH_2Ph)_4]^{3-}$.

B. Magnetization. Measurements were made for seven $[Fe_4S_4(SR)_4]^{3-}$ salts in the solid state at 4.2 K and for two of these salts at 1.45 K. The magnetic field dependencies of the magnetization per cluster, in Bohr magnetons at 4.2 K, are plotted in Figure 8 for five compounds. The magnetic moment per cluster is $M = g\mu_B\langle S_z\rangle$, where g is the average g value and $\langle S_z\rangle$ is the thermal average of the component of spin parallel to the applied field. For a paramagnet with spin S,[25] $\langle S_z\rangle = SB_S(g\mu_BH/kT)$, where $B_S(H/T)$ is the Brillouin function of the argument S. In the absence of zero field splittings, population of other spin states, or magnetic field mixing of higher lying states into the ground state wave function, $\langle S_z\rangle$ is a function of H/T only. Typically for simple paramagnets linear behavior is observed at $H/T \lesssim 2$ kOe/K and the limit $\langle S_z\rangle = S$ is asymptotically approached at $H/T \gtrsim 15$-20 kOe/K. In agreement with the low-field susceptibility data, the magnetization results show that the clusters in the solid state exhibit more complicated behavior. Values of M increase with increasing field up to $H/T \cong 13$ kOe/K at 4.2 K and, for the Et_4N^+ salts of $[Fe_4S_4(SPh)_4]^{3-}$ and $[Fe_4S_4(SCH_2Ph)_4]^{3-}$, up to $H/T = 37$ kOe/K at 1.45 K. Furthermore, M vs. H/T

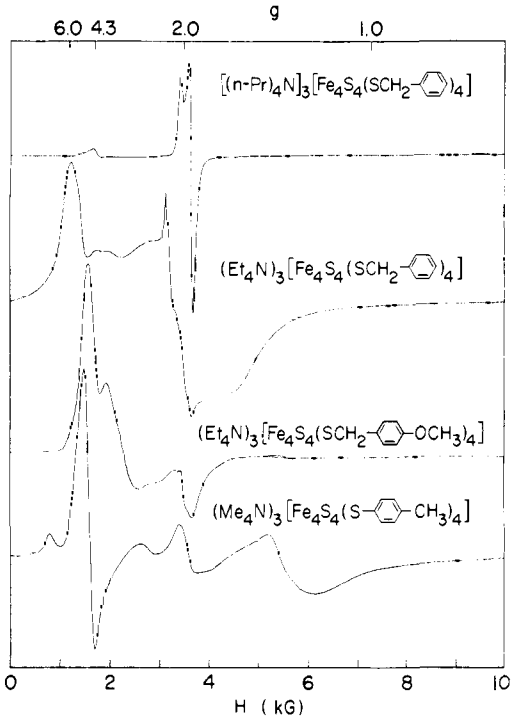

Figure 9. Solid-state X-band EPR spectra of $[Fe_4S_4(SR)_4]^{3-}$ salts at 4.2 K recorded under the following conditions of modulation amplitude (G), microwave power (mW), and receiver gain: $[(n\text{-}Pr)_4N]_3[Fe_4S_4(SCH_2Ph)_4]$, 20, 5, 1000; $(Et_4N)_3[Fe_4S_4(SCH_2Ph)_4]$, 10, 3, 20; $(Et_4N)_3[Fe_4S_4(SCH_2\text{-}p\text{-}C_6H_4OMe)_4]$, 40, 5, 200; $(Me_4N)_3[Fe_4S_4(S\text{-}p\text{-}C_6H_4Me)_4]$, 20, 5, 800. The modulation frequency in all cases was 10^5 Hz.

plots for the latter two compounds at 4.2 and 1.45 K (not shown) are not coincident.

Although the magnetization properties, as the susceptibility data, cannot yet be interpreted in detail, they reveal that the seven compounds examined fall into two categories. At the highest H/T value at 4.2 K $(Et_4N)_3[Fe_4S_4(SPh)_4]$ and $(Me_4N)_3[Fe_4S_4(S\text{-}o\text{-}C_6H_4Me)_4]$ show $M/\mu_B = 0.66$ and 0.93, respectively; the former compound has $M/\mu_B = 0.86$ at 1.45 K. These two compounds appear to be approaching the limit $M = 1\ \mu_B$ corresponding to a predominantly $S = \frac{1}{2}$ ground state assuming $g = 2$. For the other five compounds M/μ_B results at the highest H/T values are 1.46–2.34. The lower and upper limits of the range are given by $(Et_4N)_3[Fe_4S_4(S\text{-}p\text{-}C_6H_4\text{-}i\text{-}Pr)_4]$ and $(Et_4N)_3[Fe_4S_4(SCH_2\text{-}p\text{-}C_6H_4OMe)_4]$, respectively; data for the three additional compounds placed in this category are plotted in Figure 8. At $H/T \cong 37$ kOe/K at 1.45 K $(Et_4N)_3[Fe_4S_4(SCH_2Ph)_4]$ exhibits $M/\mu_B = 2.48$ and thus appears to be approaching the saturation limit of $M = 3\ \mu_B$ corresponding to a predominantly $S = \frac{3}{2}$ ground state, as does $(Et_4N)_3[Fe_4S_4(SCH_2\text{-}p\text{-}C_6H_4OMe)_4]$ at 4.2 K. The remaining three compounds in this category, $(Me_4N)_3[Fe_4S_4(SR)_4]$ (R = *m*-, *p*-C_6H_4Me) and $(Et_4N)_3[Fe_4S_4(S\text{-}p\text{-}C_6H_4\text{-}i\text{Pr})_4]$, much less closely approach this limit but clearly have magnetization properties more nearly similar to $(Et_4N)_3[Fe_4S_4(SCH_2Ph)_4]$ than to the two compounds having $M/\mu_B < 1$. The division of these seven compounds based on magnetization behavior correlates with that proposed from magnetic susceptibility results.

EPR Spectra. X-Band spectra of the nine cluster trianion salts in Table II were determined at ~4.2 K in the solid state and in frozen solutions. Results in the solid state are considered first. The types of spectra observed are encompassed by the examples provided in Figure 9 and may be divided into two sharply distinct categories: nearly isotropic or axially symmetric, with absorption in the ca. 3000–3800 G range; complex, with absorption extending over a range as large as ca. 500–7000 G. The first category contains four compounds, the Et_3MeN^+ and Et_4N^+ salts of $[Fe_4S_4(SPh)_4]^{3-}$, $(n\text{-}Pr_4N)_4[Fe_4S_4(SCH_2Ph)_4]$, and $(Me_4N)_3[Fe_4S_4(S\text{-}o\text{-}C_6H_4Me)_4]$. The latter has a nearly isotropic spectrum centered at $g = 1.94$, and the other three compounds display axial spectra with line widths and g values very similar to those in frozen solutions (Figure 7). The axial spectrum of $(n\text{-}Pr_4N)_3[Fe_4S_4(SCH_2Ph)_4]$ in Figure 9, with $g_\parallel = 2.05$ and $g_\perp = 1.92$, is typical. The remaining five compounds, the spectra of three of which are included in Figure 9, constitute the second category. Their spectra are spread over a larger magnetic field range and none is of the simple $S = \frac{1}{2}$ axial or rhombic type. From Table II it is seen that the two categories of EPR spectra tend to correlate with μ_1 values at 4.2 K. The first and second categories are associated with compounds having moments of ≤ 2.6 and $\geq 3.1\ \mu_B$, respectively. Particularly noteworthy in this respect is the occurrence of a different salt of the same cluster, $[Fe_4S_4(SCH_2Ph)_4]^{3-}$, in each category. The spectra suggest an essentially tetragonal structure for the clusters in compounds of the first category and a range of structures lacking axial symmetry for clusters of the second category. The complexity of these spectra implies significant population of $S \neq \frac{1}{2}$ states, in accord with susceptibility and magnetization data. In this respect these spectra display certain similarities to the spectra of a family of trans-octahedral Cr(III) complexes[26] which have proven extremely sensitive to distortions from tetragonal symmetry.

The EPR spectra of four cluster salts in the solid and frozen solution states may be compared by examination of Figures 7 and 9. For these and all other compounds the result of passing from the solid to the solution state is the same: nearly identical axial spectra[27] are observed in solution. Principal g values from these spectra are compiled in Table II. The clear implications of these results are that clusters in compounds of the first category undergo substantially less structural change in the solid → solution process than do those of the second category, and all species in solution adopt a structure affording effective axial electronic symmetry by the EPR criterion.

Discussion

On the basis of similarities and differences in their Mössbauer, magnetic susceptibility, high field magnetization, and EPR properties in the solid state the nine compounds, containing seven different $[Fe_4S_4(SR)_4]^{3-}$ clusters, can be divided into two categories. Property criteria which lead to this division and organization of the compounds in categories A and B are contained in Table IV. The designation of the compounds in category A as tetragonal follows from the elongated tetragonal core structure established in $(Et_3MeN)_3[Fe_4S_4(SPh)_4]$ by X-ray diffraction.[6] Similarly, the compounds in category B are termed nontetragonal (i.e., possessing less than axial core symmetry) based on the X-ray structure of $(Et_4N)_3[Fe_4S_4(SCH_2Ph)_4]$.[16] The following observations are considered especially persuasive in support of the proposal that the lack of $[Fe_4S_4(SR)_4]^{3-}$ structural uniformity in the solid state, as reflected by the four sets of magnetic and spectroscopic properties, arises from environmental perturbations: (a) two salts of the same cluster, $[Fe_4S_4(SCH_2Ph)_4]^{3-}$, fall into different categories; (b) different ring methyl positions in the $[Fe_4S_4(SC_6H_4Me)_4]^{3-}$ series with a constant cation (Me_4N^+) afford one compound (R = *o*-C_6H_4Me) in category A and the other two compounds in category B; (c) Et_4N^+ salts of the pair $[Fe_4S_4(SPh)_4]^{3-}/[Fe_4S_4(S\text{-}p\text{-}C_6H_4\text{-}i\text{-}Pr)_4]^{3-}$, differing only in the ring para substituent, occur in different categories.

In the absence of additional X-ray structural results the division of compounds in Table IV represents our best attempt to organize clusters into tetragonal and nontetragonal groups. These designations apply to the Fe_4S_4 core structures. Al-

Table IV. Classification of $[Fe_4S_4(SR)_4]^{3-}$ Cluster Compounds. Spectroscopic and Magnetic Experiments and Proposed Structures in the Solid State

compd	experiments			
	Mössbauer[a]	magnetic susceptibility[c]	magnetization[a,d]	EPR[b] (X-band)
		A. Elongated Tetragonal		
$(Et_3MeN)_3[Fe_4S_4(SPh)_4]$ $(Et_4N)_3[Fe_4S_4(SPh)_4]$ $(Me_4N)_3[Fe_4S_4(S\text{-}o\text{-}C_6H_4Me)_4]$ $(n\text{-}Pr_4N)_3[Fe_4S_4(SCH_2Ph)_4]$	two overlapping quadrupole doublets; δ_1 0.50–0.52, $(\Delta E_Q)_1 \sim 1.9$–2.0, δ_2 0.43–0.45, $(\Delta E_Q)_2 \sim 1.1$ mm/s at 4.2 K	$\mu_t \sim 2.0$–2.6 μ_B at 4.2 K; $\mu_t \lesssim 3.1$ μ_B at 50 K; antiferromagnetic	$M/\mu_B \lesssim 1$ at $H/T \cong 13, 37^c$ kOe/K (T = 1.45, 4.2 K)	nearly isotropic or axial spectra (3.0–3.8 kG), g values 1.92–1.94, 2.05–2.07
		B. Nontetragonal		
$(Et_4N)_3[Fe_4S_4(SCH_2Ph)_4]$ $(Me_4N)_3[Fe_4S_4(S\text{-}m\text{-}C_6H_4Me)_4]$ $(Me_4N)_3[Fe_4S_4(S\text{-}p\text{-}C_6H_4Me)_4]$ $(Et_4N)_3[Fe_4S_4(S\text{-}p\text{-}C_6H_4\text{-}i\text{-}Pr)_4]$ $(Et_4N)_3[Fe_4S_4(SCH_2\text{-}p\text{-}C_6H_4OMe)_4]$	broadened quadrupole doublets; δ 0.43–0.48, $\Delta E_Q \sim 0.9$–1.4 mm/s at 4.2 K, magnetic hyperfine splittings ~50% of those in category A	$\mu_t \sim 3.1$–3.9 μ_B at 4.2 K; $\mu_t \gtrsim 3.4$ μ_B at 50 K; antiferromagnetic	$M/\mu_B \gtrsim 1.5$ at $H/T \cong 13, 37^c$ kOe/K (T = 1.45, 4.2 K)	complex spectra extending over ca. 0.5–7 kG

[a] Seven examples. [b] Nine examples. [c] One example. [d] Saturation moments not achieved under the indicated conditions.

though not generally demonstrable with the information at hand, it is considered unlikely that a cluster containing a tetragonal core but with less than overall tetragonal symmetry would generate properties consistent with category B. Such a cluster could be realized, and, indeed, is found in $(Et_3MeN)_3[Fe_4S_4(SPh)_4]$,[6] by appropriate spatial disposition of R substituents and deformations of exterior RS–Fe–S angles.[28] Yet the cluster in this compound is the prototype member of category A. A high degree of core structural regularity within each category is not implied, but is more likely for the members of category A. The larger variations in a given property exhibited by the members of category B are interpreted in terms of a range of core structures with differing degrees of departure from idealized tetragonal core symmetry. Without further structural data it is not possible to correlate the properties of compounds in category B with the physical forms of distortions from core tetragonality.

Irrespective of their placement in category A or B, all compounds in frozen acetonitrile solution exhibit nearly coincident Mössbauer and EPR spectra (Tables I and II), and three compounds have similar magnetic moments at 4.2 K and $\mu_t(T)$ behavior up to 150 K. Further, in fluid acetonitrile solution (230–304 K) μ_t values of the Et_4N^+ salts of $[Fe_4S_4(SPh)_4]^{3-}$ and $[Fe_4S_4(SCH_2Ph)_4]^{3-}$, category A and B solids, respectively, are the same within experimental error.[19] Collectively these observations provide convincing evidence that $[Fe_4S_4(SR)_4]^{3-}$ species adopt in solution a constant core structure, or a range of closely related core structures which are not clearly distinguishable by the methods employed here. Core structural changes between solid and solution phases, shown earlier for $(Et_4N)_3[Fe_4S_4(SCH_2Ph)_4]$ only,[6] can now be considered a general occurrence for compounds whose properties place them in category B. From the previous demonstration[6] that solution and solid-state properties of $[Fe_4S_4(SPh)_4]^{3-}$ are virtually identical, the core structure in solution is identified as the elongated tetragonal D_{2d} configuration II in Figure 1. Inasmuch as a frozen solution is less likely to provide perturbing influences than a crystalline state, and seven different $[Fe_4S_4(SR)_4]^{3-}$ species have now been shown to adopt this or a very similar structure, proposal (1), given at the outset, enjoys broad experimental support. An equivalent base of support (including the uniform core structures of $[Fe_4S_4(SR)_4]^{2-}$ [7,14,15]) then follows directly for proposal (2). The process I $\rightleftharpoons$ II, which is described in more detail elsewhere,[6] provides only a small reorganization barrier to electron exchange as evidenced by the self-exchange rate of $\sim 10^6$ M^{-1} s^{-1} for $[Fe_4S_4(S\text{-}p\text{-}C_6H_4Me)_4]^{2-,3-}$ in acetonitrile solution at 25 °C.[29]

With the process I $\rightleftharpoons$ II in Figure 1 now established as the unconstrained structural change accompanying electron transfer, the question arises as to whether this same change occurs in isoelectronic Fd_{ox}/Fd_{red} couples. Because of the absence of structural information and the limited physicochemical properties reported for Fd_{red} proteins, this question can be addressed only indirectly. Comparison of available physicochemical properties of $[Fe_4S_4(SR)_4]^{3-}$ species and Fd_{red} proteins in solution,[4-6] while sufficient to show that the former are site analogues of the latter, are inconclusive with regard to inference of the core geometry of Fd_{red} sites. EPR spectra of Fd_{red} proteins in their native conformations indicate (with one exception) nonaxial site symmetry,[6] but owing to the high structural sensitivity of the technique it is unclear that such spectra reflect a significant departure of the core from the configuration II. Departure of one or both sites in a Fd_{ox}/Fd_{red} couple from the unconstrained configuration I/II would be expected to shift redox potentials from the intrinsic value of ca. −0.50 V, established by measurement of several aqueous $[Fe_4S_4(SR)_4]^{2-,3-}$ couples containing SR groups electronically similar to cysteinate residues.[30] Such an effect could contribute to the range of protein potentials reported (−0.28 to −0.49 V[30a]), as could extrinsic environmental influences on the sites.[31] We have also suggested[6] the possibility that in the native form of HP_{red} protein forces provide a structural barrier to the anisotropic core dimensional change in I $\rightleftharpoons$ II, with the result that the potential is shifted to a more negative value than in the range quoted. The HP_{red} protein is reducible in 80% Me_2SO/H_2O,[32] a medium which unfolds protein structure. Under these conditions the estimated potential is $\lesssim -0.6$ V,[32] comparable to certain Fd_{ox}/Fd_{red} and $[Fe_4S_4(SR)_4]^{2-,3-}$ potentials in the same solvent.[30a] Further assessment of site structures and their effects on properties of Fd and HP proteins is perhaps best pursued by correlation with $[Fe_4S_4(SR)_4]^{3-}$ structures in the solid and solution states. A potentially feasible method is resonance Raman spectroscopy, and this possibility is under investigation.

Acknowledgment. This research was supported by NIH Grant GM-22352 at Stanford University and by the National

Science Foundation at the Francis Bitter National Magnet Laboratory.

References and Notes

(1) (a) Stanford University; (b) Francis Bitter National Magnet Laboratory.
(2) R. H. Holm and J. A. Ibers in "Iron-Sulfur Proteins", Vol. III, W. Lovenberg, Ed., Academic Press, New York, 1977, Chapter 7.
(3) R. H. Holm, *Acc. Chem. Res.*, **10**, 427 (1977).
(4) J. Cambray, R. W. Lane, A. G. Wedd, R. W. Johnson, and R. H. Holm, *Inorg. Chem.*, **16**, 2565 (1977).
(5) R. W. Lane, A. G. Wedd, W. O. Gillum, E. J. Laskowski, R. H. Holm, R. B. Frankel, and G. C. Papaefthymiou, *J. Am. Chem. Soc.*, **99**, 2350 (1977).
(6) E. J. Laskowski, R. B. Frankel, W. O. Gillum, G. C. Papaefthymiou, J. Renaud, J. A. Ibers, and R. H. Holm, *J. Am. Chem. Soc.*, **100**, 5322 (1978).
(7) B. A. Averill, T. Herskovitz, R. H. Holm, and J. A. Ibers, *J. Am. Chem. Soc.*, **95**, 3523 (1973).
(8) (a) G. Palmer in "The Enzymes", Vol. XII, Part B, 3rd ed., P. D. Boyer, Ed., Academic Press, New York, 1975, pp 1–56; (b) D. O. Hall, R. Cammack, and K. K. Rao in "Iron in Biochemistry and Medicine", A. Jacobs and M. Worwood, Ed., Academic Press, New York, 1974, Chapter 8.
(9) (a) C. L. Hill, D. J. Steenkamp, R. H. Holm, and T. P. Singer, *Proc. Natl. Acad. Sci. U.S.A.*, **74**, 547 (1977); (b) D. J. Steenkamp, T. P. Singer, and H. Beinert, *Biochem. J.*, **169**, 361 (1978).
(10) (a) W. O. Gillum, L. E. Mortenson, J.-S. Chen, and R. H. Holm, *J. Am. Chem. Soc.*, **99**, 584 (1977); (b) D. L. Erbes, R. H. Burris, and W. H. Orme-Johnson, *Proc. Natl. Acad. Sci. U.S.A.*, **72**, 4795 (1975); (c) E. C. Hatchikian, M. Bruschi, and J. LeGall, *Biochem. Biophys. Res. Commun.*, **82**, 451 (1978).
(11) (a) G. B. Wong, D. M. Kurtz, Jr., R. H. Holm, L. E. Mortenson, and R. G. Upchurch, *J. Am. Chem. Soc.*, **101**, 3078 (1979); (b) W. H. Orme-Johnson, L. C. Davis, M. T. Henzl, B. A. Averill, N. R. Orme-Johnson, E. Münck, and R. Zimmerman in "Recent Developments in Nitrogen Fixation", W. Newton, J. R. Postgate, and C. Rodriguez-Barrueco, Eds., Academic Press, New York, 1977, pp 131–178; (d) R. Zimmerman, E. Münck, W. J. Brill, V. K. Shah, M. T. Henzl, J. Rawlings, and W. H. Orme-Johnson, *Biochim. Biophys. Acta*, **537**, 185 (1978); (e) J. R. Bale, J. Rawlings, B. A. Averill, and W. H. Orme-Johnson, results to be published; (f) D. M. Kurtz, Jr., R. S. McMillan, B. K. Burgess, L. E. Mortenson, and R. H. Holm, *Proc. Natl. Acad. Sci. U.S.A.*, in press.
(12) (a) E. T. Adman, L. C. Sieker, and L. H. Jensen, *J. Biol. Chem.*, **251**, 3801 (1976); (b) C. W. Carter, Jr., in ref 2, Chapter 6; (c) C. W. Carter, Jr., *J. Biol. Chem.*, **252**, 7802 (1977).
(13) B.-K. Teo, R. G. Shulman, G. S. Brown, and A. E. Meixner, *J. Am. Chem. Soc.*, in press.
(14) L. Que, Jr., M. A. Bobrik, J. A. Ibers, and R. H. Holm, *J. Am. Chem. Soc.*, **96**, 4168 (1974).
(15) (a) $[Fe_4S_4(SCH_2CH_2CO_2)_4]^{6-}$: H. L. Carrell, J. P. Glusker, R. Job, and T. C. Bruice, *J. Am. Chem. Soc.*, **99**, 3683 (1977). (b) $[Fe_4S_4Cl_4]^{2-}$: M. A. Bobrik, K. O. Hodgson, and R. H. Holm, *Inorg. Chem.*, **16**, 1851 (1977). (c) $[Fe_4Se_4(SPh)_4]^{2-}$: M. A. Bobrik, E. J. Laskowski, R. W. Johnson, W. O. Gillum, J. M. Berg, K. O. Hodgson, and R. H. Holm, *ibid.*, 17, 1402 (1978).
(16) J. M. Berg, K. O. Hodgson, and R. H. Holm, *J. Am. Chem. Soc.*, **101**, 4586 (1979).
(17) E. A. Bartkus, E. B. Hotelling, and M. B. Neuworth, *J. Org. Chem.*, **25**, 232 (1960).
(18) H. Gilman and H. S. Broadbent, *J. Am. Chem. Soc.*, **69**, 2053 (1947).
(19) J. G. Reynolds, E. J. Laskowski, and R. H. Holm, *J. Am. Chem. Soc.*, **100**, 5315 (1978).
(20) B. V. DePamphilis, B. A. Averill, T. Herskovitz, L. Que, Jr., and R. H. Holm, *J. Am. Chem. Soc.*, **96**, 4159 (1974).
(21) C. Y. Yang, K. H. Johnson, R. H. Holm, and J. G. Norman, Jr., *J. Am. Chem. Soc.*, **97**, 6596 (1975).
(22) (a) H. Eicher, F. Parak, L. Bogner, and K. Gersonde, *Z. Naturforsch. C*, **29**, 683 (1974); (b) D. P. E. Dickson, C. E. Johnson, C. L. Thompson, R. Cammack, M. C. W. Evans, D. O. Hall, K. K. Rao, and U. Weser, *J. Phys. (Paris)*, **35**, C6-343 (1974); (c) P. Middleton, D. P. E. Dickson, C. E. Johnson, and J. D. Rush, *Eur. J. Biochem.*, **88**, 135 (1978).
(23) In addition to different magnitudes and directions of the magnetic hyperfine interactions at the two sites, the overall complexity of this and other $[Fe_4S_4(SR)_4]^{3-}$ spectra obtained in applied fields arises from different quadrupole interactions, randomization in the powder sample of the angle between the principal component of the electric field gradient and the magnetic hyperfine field, and possible asymmetries in both the quadrupole and magnetic hyperfine interactions.
(24) Structural differences would be expected to influence the exchange interactions leading to antiparallel spin alignment and, thus, the energies of the spin states of the clusters. In this event it is reasonable that magnetic properties would differ most at low temperatures where energy spacings may be comparable to kT. Development of a spin-coupling model for the $[Fe_4S_4]^+$ core of trianions as a means of interpreting $\chi_t(T)$ behavior is in progress.
(25) For further details cf., e.g., R. L. Carlin and A. J. van Duyneveldt, "Magnetic Properties of Transition Metal Compounds," Springer-Verlag, New York, 1977, Chapter I.
(26) E. Pederson and H. Toftlund, *Inorg. Chem.*, **13**, 1603 (1974).
(27) The lesser resolution between the axial signals in the lower two compared to the upper two spectra in Figure 7 is likely due to a larger concentration of a radical impurity with $g = 2.00$.[6] This impurity occurs in varying degrees in all isolated cluster trianion salts, and its presence in the salt of $[Fe_4S_4(SCH_2\text{-}p\text{-}C_6H_4OMe)_4]^{3-}$ is indicated by the partially resolved sharp feature at $g = 2.0$ in Figure 9. Spectra of all $[Fe_4S_4(SR)_4]^{3-}$ species are axial in DMF. Axial spectra are observed in acetonitrile for all species but those with R = Ph and *o*-, *m*-, *p*-C_6H_4Me. In these cases a nearly isotropic spectrum centered at $g \cong 1.94$ is found with the same line width in CH_3CN and CD_3CN. Addition of DMF to $\lesssim 50\%$ v/v produces well-resolved axial spectra. The solvent effects on spectra were observed at 4.2 K and have not been further examined.
(28) In the compound cited the Fe_4S_4 core has idealized tetragonal symmetry, which divides the 12 RS–Fe–S angles into "symmetry-related" sets of 8 and 4. Ranges of values of these angles are 109.5–123.6 and 98.3–114.2° (anion 1[6]), respectively, which serve to emphasize the departure of the entire cluster from tetragonal symmetry.
(29) J. G. Reynolds, C. L. Coyle, and R. H. Holm, results to be published.
(30) (a) C. L. Hill, J. Renaud, R. H. Holm, and L. E. Mortenson, *J. Am. Chem. Soc.*, **99**, 2549 (1977). (b) Another estimate of the intrinsic potential is −0.6 V; cf. R. C. Job and T. C. Bruice, *Proc. Natl. Acad. Sci. U.S.A.*, **72**, 2478 (1975).
(31) E. Adman, K. D. Watenpaugh, and L. H. Jensen, *Proc. Natl. Acad. Sci. U.S.A.*, **72**, 4854 (1975); R. J. Kassner and W. Yang, *J. Am. Chem. Soc.*, **99**, 4351 (1977).
(32) R. Cammack, *Biochem. Biophys. Res. Commun.*, **54**, 548 (1973).